Northern Hemisphere Snow Extent Derived from Microwave and Optical Satellite Data

Richard L. Armstrong and Mary Jo Brodzik
National Snow and Ice Data Center
Cooperative Institute for Research in Environmental Sciences
University of Colorado, Boulder, Colorado, USA

Introduction

The extent and variability of seasonal snow cover are important parameters in large-scale climate and hydrologic systems. Satellite remote sensing offers the opportunity to monitor and evaluate various snow parameters and processes at regional to global scales. Similar sensor configurations are typically available for aircraft use but this presentation concentrates on data from polar orbiting satellites because of the potential for monitoring snow cover at the hemispheric to global scale with daily or near-daily spatial coverage. More importantly, a few of the data sets described below provide a time series of sufficient length to evaluate climate patterns and climate change.

Visible-band satellite data

Snow cover is often easily identifiable in visible-band satellite images because it typically possesses an albedo which exceeds most all other land surface types. Snow may be identified manually by noting the magnitude of the reflectance or it may be identified automatically by the application of an algorithm which recognizes the specific spectral signature of snow. For example, at wavelengths above 1.4 um the reflectance of snow amounts to only a few percent enabling good discrimination between snow and clouds since the reflectance of clouds remains high at that wavelength (Wiscombe and Warren, 1981).

Some of the earliest applications of satellite remote sensing involved efforts to map and monitor the areal extent of snow cover. In fact, snow cover extent is the longest available environmental product provided by satellite remote sensing. In 1966 the National Oceanographic and Atmospheric Administration (NOAA) began an operational program to map Northern Hemisphere snow extent using available visible-band satellite data (Matson *et al.*, 1986; Robinson *et al*., 1993). Within the next ten years researchers began to present results demonstrating the operational capabilities of satellite remote sensing in snow hydrology (Schneider *et al*., 1976; Rango, 1975).

During the past four decades much important information on continental to hemispheric scale snow extent has been provided by satellite remote sensing in the visible wavelengths. From 1966 to 1999 NOAA-NESDIS produced weekly snow extent charts for Northern Hemisphere land surfaces using visible-band satellite imagery (Robinson *et al*., 1993; Frei and Robinson, 1999). These NOAA charts were derived from the manual interpretation of Advanced Very High-Resolution Radiometer (AVHRR), Geostationary Operational Environmental Satellite (GOES), the European satellite (METEOSAT) and Japan's geostationary meteorological satellites and other visible satellite data. The charts were then digitized on a weekly basis using an 89 by 89 Northern Hemisphere polar stereographic grid with a nominal resolution of 190.5 km. The data values are binary and grid cells are classified as snow-covered or snow-free if the cell has more or less than 50% snow cover (Dewey and Heim, 1982).

In 1997, NOAA-NESDIS began the process of migrating to a more automated procedure for generating a daily, higher resolution (1024 by 1024 polar stereorgraphic grid with a resolution of approximately 25 km) snow cover analysis as the coarse resolution of the weekly charts had been shown to cause errors in the National Meteorological Center's Numerical Weather Prediction (NWP) models. The result was the Interactive Multisensor Snow and Ice Mapping System (IMS) which incorporates a wide variety of satellite imagery (AVHRR, GOES, SSM/I) as well as derived mapped products (USAF Snow/Ice Analysis) and surface observations and allows a trained meteorologist to produce a hemispheric analysis in one hour as opposed to 10 hours with the old weekly product (Ramsay, 1998). The new daily analysis and the old weekly product were overlapped for two winters to determine if the switch introduced any inhomogeneity into the existing weekly product (Robinson *et al*., 1999). The weekly product was phased out on June 1 1999, but a "pseudo-weekly" map is generated by taking the Sunday IMS map and interpolating this back to the coarse resolution of the earlier weekly product.

To facilitate the use of these data, the National Snow and Ice Data Center (NSIDC) University of Colorado, has developed the Northern Hemisphere EASE-Grid Weekly Snow Cover and Sea Ice Extent Version 3 (Armstrong and Brodzik, 2005), a northern hemisphere cryospheric product which combines snow cover and sea ice extent at weekly intervals (Figure 1.). The snow data set is based on the weekly NOAA charts, revised by Robinson *et al*. (1993), for the period 1966 to present, while the sea ice data set, based on passive microwave remote sensing covers the period 1978 to present. This data set also includes monthly climatologies describing snow and sea ice extent in terms of average conditions, probability of occurrence, and variance. The data set is produced in a 25 km azimuthal equal area projection (NSIDC Equal Area Scalable Earth Grid or EASE-Grid) and is updated at frequent intervals. (http://nsidc.org)

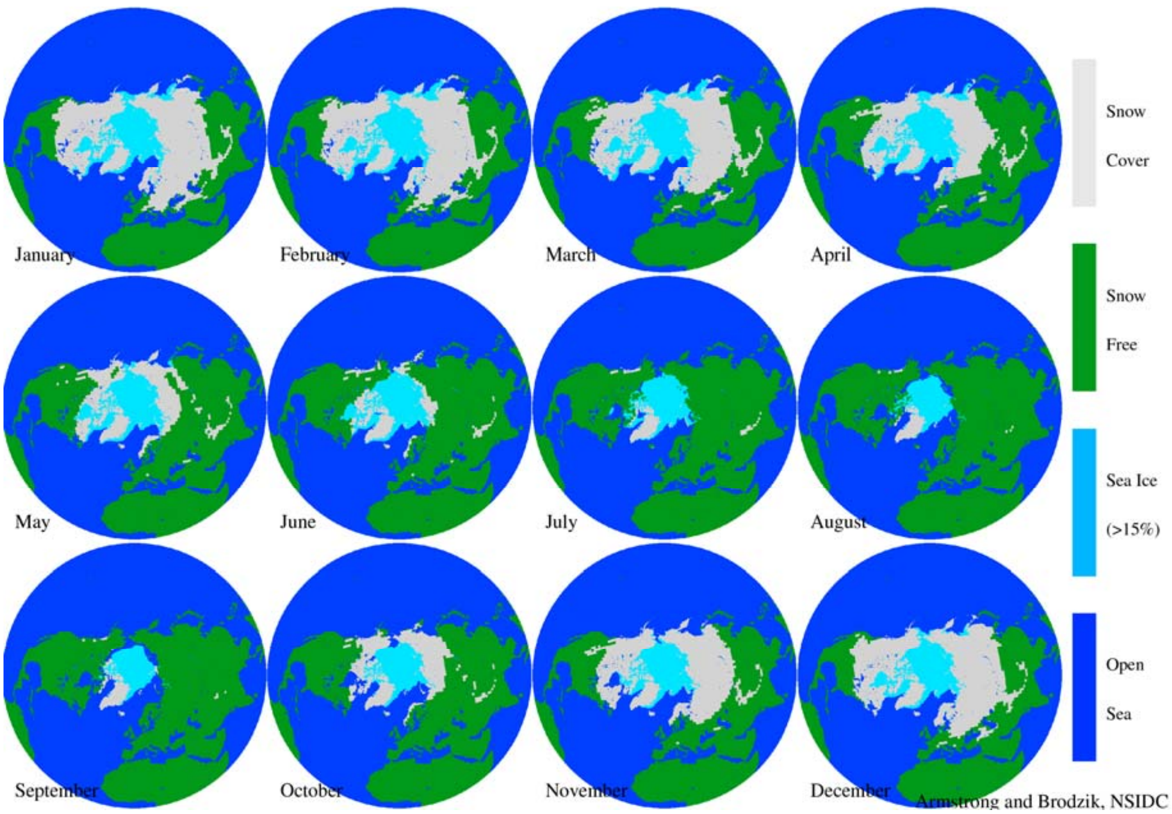

Figure 1. Monthly Northern Hemisphere snow cover (1966-2006) and sea ice extent (1978-2006) climatologies.

Passive microwave satellite data

Because of the ability to penetrate clouds, provide data during darkness and the potential to provide an index of snow depth or water equivalent, passive microwave satellite remote sensing can greatly enhance snow measurements based on visible data alone. Reliable, multichannel, global, passive microwave satellite data first became available with the NASA SMMR (Scanning Multichannel Microwave Radiometer) instrument during the period 1978-1987 (Gloersen *et al*., 1984; Hall and Martinec, 1985), followed by the DMSP (Defense Meteorological Satellite Program) SSM/I (Special Sensor Microwave/Imager) from 1987 to 2007 and beyond (Hollinger *et al*., 1990). The SMMR and SSM/I instruments provided a combined range of microwave frequencies from 6 to 89 GHz in both horizontal and vertical polarizations. Techniques used to derive snow parameters from passive microwave data have relied most heavily on channels at 18-19, 37 and 85 GHz. When snow covers the ground, the microwave energy emitted by the underlying soil is scattered by the snow grains. Therefore, when moving from snow-free to snow-covered land surfaces, a sharp decrease in emissivity and associated brightness temperature provides an indication of the presence of dry snow (Mätzler, 1994). Brightness temperature is the product of emissivity at the given microwave frequency and the physical temperature of the target (Staelin *et. al*, 1977). In addition, snow exhibits a negative spectral gradient which means that as the microwave frequency increases, for example from 19 to 37 GHz, the emissivity and associated brightness temperatures decrease. Nearly all other land surface types exhibit a positive spectral gradient. Theoretical and empirical studies have demonstrated that the amount of scattering, or decrease in brightness temperature, can be correlated with the thickness and density of the snow cover. Based on these relationships, algorithms have been developed which indicate the presence of snow (Grody and Basist, 1996) and compute either snow water equivalent or depth, given an assumed density (examples include, Chang *et al*., 1987; Goodison, 1989; Nagler, 1991; Tait, 1998; Pulliainen and Hallikainen, 2001). Nearly all of these algorithms have been developed and tested for dry snow conditions only. Snow water equivalent cannot be determined when the snow is wet (i.e. liquid water is present on the snow grain surface) because wet snow is primarily an emitter at microwave frequencies and thus the information derived from the scattered portion of the signal is lost. However, it is still possible to detect the presence of wet snow due to its high polarization difference (Walker and Goodison, 1993; Mätzler, 1994).

Comparison of visible and passive microwave data records and trends

In the comparisons shown here (Figure 2.) the Chang *et al.* (1987) algorithm is used to determine snow extent for the SMMR period and a modified version of the same algorithm is used for the SSM/I period (Armstrong and Brodzik, 2001a). Figure 2 shows the similar inter-annual variability of the two data sets where both consistently indicate Northern Hemisphere maximum extents exceeding 40 million km^2. Figure 3 compares mean monthly Northern Hemisphere snow extent for the period 1978 to 2006 and shows the difference between the two data sets. The microwave data indicate less snow-covered area than the visible data throughout the year with a mean difference during the winter months (November-April) of about 4 million square kilometers, decreasing from about 8 million square kilometers (twenty-five percent) in November to about 0.3 million square kilometers (one percent) in April (Armstrong and Brodzik, 2001a,b). It is likely that the large differences in snow extent during fall and early winter are due primarily to the inability of the current passive microwave algorithms to detect thin and intermittent snow cover. There is no reason to expect that the NOAA data would overestimate snow extent during fall and early winter.

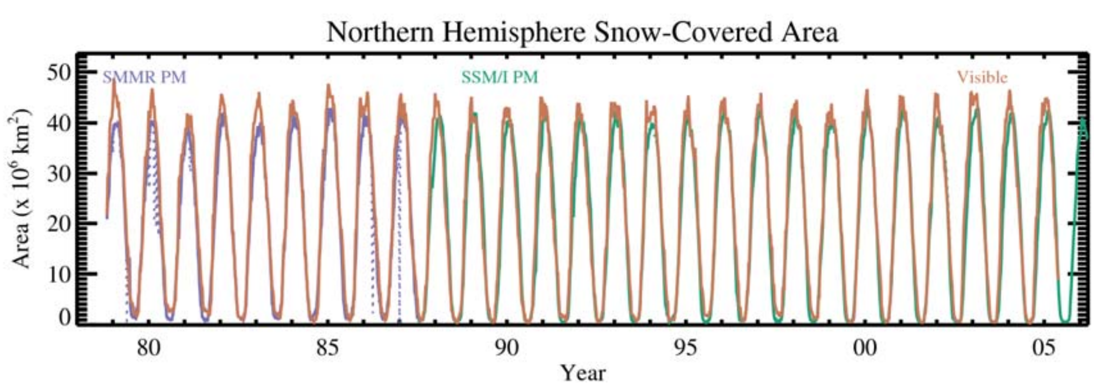

Figure 2. Northern Hemisphere monthly SCA, 1978-2006, from NOAA snow charts (orange) and microwave satellite (purple/green) data sets.

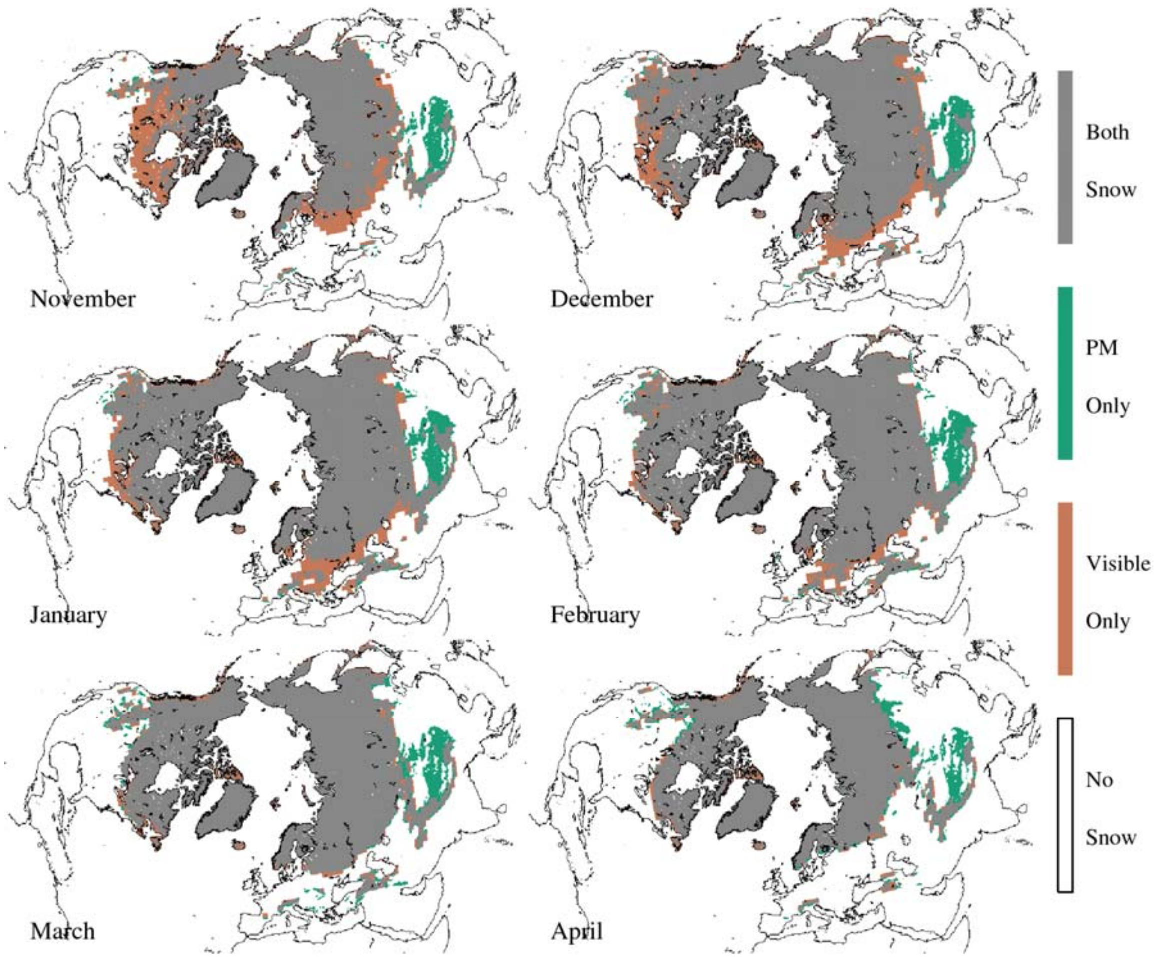

Figure 3. Comparison of mean monthly Northern Hemisphere snow extent derived from visible and passive microwave satellite data, 1978–2006 (50% or more of the weeks in the particular month over the total time period classified as snow covered).

The Tibet Plateau is the only large geographic region in the Northern Hemisphere where the microwave retrievals tend to consistently overestimate snow extent when compared with the snow cover climatologies derived from optical data (see Figure 3). This results primarily from the fact that most snow algorithms have been empirically tuned to perform well at lower elevations (thicker atmosphere). Using radiosonde data from both the more typical lower elevations and the exceptional Tibet Plateau, combined with a radiative transfer model, we have derived the coefficients required to make the necessary corrections to retrievals over land surfaces at high elevations. The next update of this data set will include this correction.

For the Northern Hemisphere the NOAA time series indicates a significant decreasing trend of -2.0% per decade. There is a decreasing trend of -0.7% per decade in the microwave snow cover although it is not significant at the 90% level (Figure 4.). The strongest seasonal signal occurs during May to August when both data sets indicate significant decreasing trends. This pattern makes physical sense in the context of increasing air temperatures during the period of maximum seasonal snow melt over the Northern Hemisphere. The geographic locations with the strongest decreasing trends within the satellite remote sensing data (Brodzik and Armstrong, 2006) include the western United States, which supports recent results by Groisman *et al.* (2004) and Mote *et al.* (2005) using in situ observations.

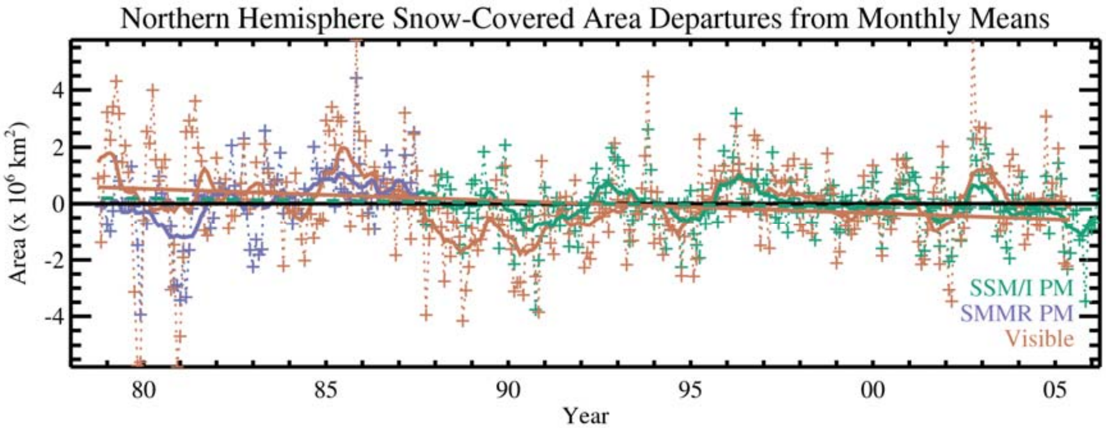

Figure 4. Northern Hemisphere SCA departures from monthly means, 1978-2006, from NOAA snow charts (orange) and microwave satellite (purple/green) data sets. The NOAA time series for this period exhibits a significant decreasing trend of -2.0% per decade (solid orange line); the microwave snow cover time series exhibits a decreasing trend of -0.7% per decade that is not significant at a 90% level (dashed green line).

New sensor systems

The launch of the NASA Earth Observing System (EOS) platforms of Terra in December of 1999 and Aqua in May of 2002 provided additional and enhanced opportunities for mapping of snow at the global scale. Both Terra and Aqua carry a MODIS (Moderate Resolution Imaging Spectroradiometer) which provides global snow maps at a 500 m resolution as both daily and eight day products in both a sinusoidal (500 m) and a "modelers grid" projection (0.05. deg.)(Hall *et al.*, 2001). Additional research products are also being developed which include sub-pixel snow covered area, albedo and grain size (Painter *et al.*, 2003).

The Aqua platform also carries the AMSR-E (Advanced Microwave Scanning Radiometer – EOS) which has been providing passive microwave-derived snow water equivalent at the global scale since 2002 (Kelly *et al.*, 2002). AMSR-E incorporates several enhancements to SMMR and SSM/I in that it provides twice the spatial resolution of the previous sensors as well as additional channels (AMSR-E channels are 6.9, 10.6, 18.7, 23.8, 36.5, and 98.0 GHz, all V and H pole). AMSR-E snow cover products include snow extent and snow water equivalent at a 25 km spatial resolution. Data are available for both Northern and Southern Hemisphere at three time intervals, daily, weekly maximum and monthly average. These standard MODIS and AMSR-E snow products are available from NSIDC (http://nsidc.org). As noted above, there are clear advantages and corresponding disadvantages in applying only visible or passive microwave methods to snow mapping, thus newer products represent a blend of both MODIS and AMSR-E (Armstrong *et al.*, 2005). For MODIS and AMSR-E sensor specifications, see Appendix A.

References:

Armstrong, R.L., Brodzik, M.J., Knowles, K. and Savoie, M. (2005). Global monthly EASE-Grid snow water equivalent climatology. Boulder, Colorado, National Snow and Ice Data Center. Digital media.

Armstrong, R.L. and Brodzik, M.J. (2005). Northern Hemisphere EASE-Grid weekly snow cover and sea ice extent version 3, Boulder, Colorado, National Snow and Ice Data Center. Digital media.

Armstrong, R.L. and Brodzik, M.J. (2001a). Recent Northern Hemisphere snow extent: a comparison of data derived from visible and microwave sensors, *Geophys. Res. Letters*, **28**, No.19:3673-3676.

Armstrong, R.L. and Brodzik, M.J. (2001b). Validation of Passive Microwave Snow Algorithms, Remote Sensing and Hydrology 2000, IAHS Pub. No. 267, eds. M. Owe, K. Brubaker, J. Ritchie and A. Rango,

Brodzik, M.J., Armstrong, R. L., Weatherhead, E.C., Savoie, M.H., Knowles, K.W. and Robinson, D. A. (2006). Regional trend analysis of satellite-derived snow extent and global temperature anomalies. EOS Transactions AGU, 87(52), fall Meeting Supplement. Abstract U33A-0011.

Chang, A.T.C., Foster, J. L. and Hall, D.K. (1987). Nimbus-7 SMMR derived global snow cover parameters.

Ann. Glaciol., **9**, 39-44.
Dewey, K.F. and Heim, Jr., R. (1982). A digital archive of Northern Hemisphere snow cover, November 1966 through December 1980. *Bull. Amer. Met. Soc.*, **63**, 1132-1141.
Frei, A. and Robinson, D.A. (1998). Evaluation of snow extent and its variability in the Atmospheric Model Intercomparison Project. *J. Geophys. Res. - Atmospheres*, **103** (D8), 8859-8871.
Gloersen, P., Cavalieri, D. J.,Chang, A. T.C., Wilheit, T.T., Campbell, W. J., Johannessen, O. M., Katsaros, K. B., Kunzi, K. F.,Ross, D. B., Staelin, D., Windsor, E. P. L., Barath, F. T. Gudmandsen, P., Langham, E., Ramseier, R. O. (1984). A summary of results from the first Nimbus 7 SMMR observations. Journal of Geophysical Research, **89** (D4): 5335-5344
Goodison, B.E. (1989). Determination of areal snow water equivalent on the Canadian prairies using passive microwave satellite data. *IGARSS'89*, 12th Canadian Symposium on Remote Sensing, Vancouver, Canada, July 10-14, 1989. Vol. 3, pp. 1243-1246.
Grody, N. C. and Basist, A. (1996). Global identification of snow cover using SSM/I measurements. IEEE Trans. Geosci. Remote Sens. , GE-34 (1), pp. 237-249.
Groisman, P. Ya., Karl, T.R. Easterling, D.R., Sun, B. and Lawrimore, J.H. (2004). Contemporary changes of the hydrological cycle over the contiguous United States: trends derived from in situ observations. *J. Hydrometeorol.,* **5**, 64-85.
Hall, D.K., Riggs, G.A., Salomonson, V.V. and Scharfen, G.R. (2001). Earth Observing Sysstem (EOS) moderate resolution imaging spectroradiometer (MODIS) global snow cover products. *IAHS Publ. No. 267*, pp. 55-60.
Hall D.K. and Martinec, J. (1985). *Remote Sensing of Ice and Snow*, New York: Chapman and Hall.
Hollinger, J.P., Pierce, J.L. and Poe, G.A. (1990). SSM/I instrument evaluation. *IEEE Trans.Geosci. Remote Sens.,* **28**(5), 781-790
Kelly, R., A. Chang, L. Tsang and J. Foster. 2002. Development of a prototype AMSR-E global snow area and snow volume algorithm. IEEE Transactions on Geoscience and Remote Sensing, **41**:230-242.
Matson, M., Ropelewski, C.F. and Varnadore, M.S. (1986). *An Atlas of Satellite-derived Northern Hemisphere Snow Cover Frequency,* NOAA, Washington, D.C., 75 p.
Mätzler, C. (1994). Passive microwave signatures of landscapes in winter. *Meteorol. Atmos. Phys.,* **54**, 241-260.
Mote, P.W., A.F. Hamlet, M.C. Clark and D.P. Lettenmaier. (2005). Declining mountain snowpack in western North America. Bull. Am. Met. Soc. **86** (1):39-49.
Nagler, T. (1991). Verfahren zur Analyse der Schneebedeckung aus Messungen des SSM/I. (Diplomarbeit thesis, University of Innsbruck)
Painter, T.H., Dozier J., Roberts, D.A., Davis, R.E. and Green, R.O. (2003). Retrieval of subpixel snow-covered area and grain size from imaging spectrometer data. *Remote Sensing of Environment*, 85, 64-77.
Pulliainen, J. and Hallikainen, M. (2001). Retrieval of regional snow water equivalent from space-borne passive microwave observations, *Remote Sens. Environ.*, **75**, 76-85.
Rango, A. ed. (1975). *Proceedings of the Workshop on Operational Applications of Satellite Snowcover Observations*, National Aeronautics and Space Administration, Washington, D.C. NASA SP39.
Ramsay, B.H. (1998). The Interactive Multisensor Snow and Ice Mapping System. *Hydrol. Processes*, **12**, 1537-1546.
Robinson, D.A., Dewey, K.F. and Heim, R.R. (1993). Global snow cover monitoring: an update. *Bull. Am. Meteorol. Soc.*, **74**, 1689-1696.
Robinson, D.A., Tarpley, J.D. and Ramsay, B.H. (1999). Transition from NOAA weekly to daily hemispheric snow charts. *Am. Met. Soc. 10th Symposium on Global Change Studies*, Dallas, TX, January, 1999, pp. 487-489.
Schneider, S.R., Wiesnet, D.R. and McMillan, M.C. (1976). River basin snow mapping at the National Environmental Satellite Service, *NOAA Tech. Memo. NESS 83*, Washington, DC: U.S. Department of Commerce.
Staelin, D.H., Rosenkrnaz, P.W., Barath, F.T., Johnston, E.J. and Waters, J.W. (1977). Microwave spectroscopic imagery of the Earth. *Science*, **197,** 991-993.
Tait, A. (1998). Estimation of snow water equivalent using passive microwave radiation data. *Remote Sens. Environ.,* **64**, 286-291.
Walker, A.E. and Goodison, B.E. (1993). Discrimination of wet snow cover using passive microwave satellite data. *Ann. Glaciol.*, **17**, 307-311.
Wiscombe, W.J. and Warren, S.G. (1981). A model for the spectral albedo of snow. I. Pure snow. *J. Atmos. Sci.*

37, 2712-2733.

Appendix A. NASA-EOS Operational data streams -

AMSR-E snow cover products: snow water equivalent

a. Frequency of product availability: daily, five-day, monthly

b. Delay between time of observation and product availability: 48 hours for preliminary data, 4 days for official products.

c. Period of record covered :18 June 2002 – present (no significant time gaps)

d. File format details: Hierarchical Data Format - Earth Observing System (HDF-EOS) format – see http://nsidc.org/data/ae_dysno.html

e. Compatibility with commonly used GIS or image processing software – 721 x 721 equal area projection, 25 km x 25 km grid, see http://nsidc.org/data/ae_dysno.html

f. Characterization of weaknesses or caveats – spatial resolution appropriate for large regional to hemispheric scale studies, typically not appropriate for basin-scale studies.

MODIS snow cover products: snow extent, albedo, fractional cover

a. Frequency of product availability: daily, eight-day, monthly

b. Delay between time of observation and product availability: 48 hours for daily product

c. Period of record covered : 24 February 2000 – present (no significant time gaps)

d. File format details: Hierarchical Data Format - Earth Observing System (HDF-EOS) format and geoTIFF – see http://nsidc.org/data/mod10a1.html

e. Compatibility with commonly used GIS or image processing software – 1200 km x 1200 km tiles of 500 m resolution data gridded in a sinusoidal map projection. see http://nsidc.org/data/mod10a1.htmll

f. Characterization of weaknesses or caveats – data availability will be limited in regions of persistent cloud cover.